# Turbidity hysteresis in an estuary and tidal river following an extreme discharge event

David K. Ralston[1], Brian Yellen[2], Jonathan D. Woodruff[2], Sarah Fernald[3]

[1] Woods Hole Oceanographic Institution, Woods Hole, MA, USA

[2] University of Massachusetts, Amherst, MA, USA

[3] New York State Department of Environmental Conservation, Hudson River National Estuarine Research Reserve, Staatsburg, NY, USA

dralston@whoi.edu, 508-289-2587

For *Geophysical Research Letters*

## Key points

- Turbidity-discharge relationships are found in long-term observations (≥12 years) at multiple locations along the tidal Hudson River
- In the tidal freshwater, turbidity for a given discharge increased for 2 years following major discharge events and sediment input in 2011
- In the saline estuary turbidity hysteresis was less apparent, consistent with greater background sediment concentrations and availability

## Abstract

Non-linear turbidity-discharge relationships are explored in the context of sediment sourcing and event-driven hysteresis using long-term (≥12 year) turbidity observations from the tidal freshwater and saline estuary of the Hudson River. At four locations spanning 175 km, turbidity generally increased with discharge but did follow a constant log-log dependence, in part due to event-driven adjustments in sediment availability. Following major sediment inputs from extreme precipitation and discharge events in 2011, turbidity in the tidal river increased by 20-50% for a given discharge. The coherent shifts in the turbidity-discharge relationship along the tidal river over the subsequent 2 years suggest that the 2011 events increased sediment availability for resuspension. In the saline estuary, changes in the sediment-discharge relationship were less apparent after the events, indicating that greater background turbidity due to sediment remobilization from internal sources make inputs from high discharge events less important at interannual time scales.

## Plain language summary

Turbidity is a widely accepted proxy for suspended sediment concentration and an important factor for contaminant transport and water quality. Here we show that turbidity depends on river discharge in long-term observations at multiple locations in an estuary. Such relationships are often used in rivers, but have not been commonly used in estuaries and tidal rivers where tides and salinity also contribute to variability. Turbidity in the freshwater tidal region was more sensitive to discharge than in the saline estuary. Massive inputs of sediment due to extreme precipitation and flooding in 2011 resulted in increased sediment availability in the tidal river over multiple years. Turbidity throughout the tidal river was elevated for 2 years following the events, but changes were not apparent in the saline estuary. The observations provide guidance on recovery time scales for estuaries and tidal rivers to event-driven sediment inputs, which affects the delivery of material from the watershed to the coastal ocean as well as other impacts relating to changes in turbidity.

## 1. Introduction

Due to the challenges in continuously monitoring suspended sediment concentration (SSC), SSC and sediment discharge in rivers are often empirically related to volumetric freshwater discharge (Helsel and Hirsch 2002). Volumetric discharge varies by orders of magnitude at event and seasonal time scales, and it is the dominant factor controlling variability in sediment discharge. Sediment discharge increases nonlinearly with volumetric discharge, commonly increasing to approximately the cube of river discharge at high flow (Nash 1994; Syvitski et al. 2000). Consequently, large, relatively infrequent events disproportionately contribute to the total sediment discharge.

Sediment-discharge rating curves are often treated as static, and yet variability in precipitation patterns, vegetation, land use, and tectonic activity can all affect sediment delivery and the sediment-discharge relationship (Walling 1977; Morehead et al. 2003; Warrick and Rubin 2007; Yellen et al. 2016). Disturbance from extreme floods can increase sediment concentrations for months to years as rivers adjust to bed incision and landslide scarps revegetate (Warrick et al. 2013; Dethier et al. 2016; Ahn et al. 2017; Gray 2018). The duration and timing of low-discharge conditions can also affect in-stream storage and SSC during subsequent higher discharge periods (Walling et al. 1998; Gray et al. 2014).

Rivers supply sediment to coastal regions, where sediment transport also depends on processes like tides, waves, and density-driven circulation. In estuaries, salinity gradients drive landward near-bottom circulation that leads to sediment trapping and regions of higher sediment concentration, or estuarine turbidity maximums (ETMs) (Postma 1961; Burchard et al. 2018). River discharge alters sediment input from the watershed but also affects the salinity distribution, and thus the sediment trapping at seasonal and event time scales. Tidal currents also contribute to variability in SSC, directly through sediment resuspension and indirectly by affecting the salinity distribution. In the tidal freshwater part of an estuary, tidal resuspension and sediment supply from the river are the key factors in SSC variability (Dalrymple and Choi 2007; Ralston and Geyer 2017). Tidal freshwater regions provide crucial links in the movement of material to the coastal ocean, and yet they have received less study than fluvial or estuarine environments (Hoitink and Jay 2016).

This study uses long-term (≥12-year) observations to characterize turbidity-discharge relationships in a tidal river and estuary, including the response following sediment inputs from major discharge events. Because it is easier to measure, turbidity is often used as a proxy for SSC (Yellen et al., 2014; Ahn et al., 2017), and turbidity has been shown to correlate well with SSC in the tidal river (Ralston and Geyer 2017) and within the watershed (McHale and Siemion 2014). In late summer 2011, tropical cyclones Irene and Lee delivered intense precipitation over much of the U.S. Northeast, increasing discharge and sediment delivery. In the Delaware estuary, sediment input of 1.4 Mt over about two weeks was similar to the long-term annual average, and SSC in the ETM remained elevated for several months (Sommerfield et al. 2017). In the Connecticut River estuary, input from Irene of 1.2 Mt was twice the annual average, and the sediment-discharge relationship in the tidal river was elevated for the following 2 years compared to before the storm (Yellen et al. 2014). In the Hudson River estuary, sediment input from Irene and Lee was about 2.7 Mt, more than twice the annual average (Wall et al. 2008; Ralston et al. 2013). The events increased turbidity in the months following the events, but the response to this sediment input has not been examined at longer time scales. In this study we use long-term monitoring data to assess the turbidity-discharge relationships at multiple locations along the tidal Hudson River and quantify the time scales over which the discharge events altered turbidity in the system.

## 2. Methods

### *2.1 Site description*

The Hudson River estuary extends about 265 km from the Atlantic Ocean to tidal limit at Troy (NY). Along-estuary distances in the Hudson are typically reported with respect to The Battery in New York Harbor as 0 river km (rkm), but The Battery is located about 25 km landward of the natural mouth between Sandy Hook and Rockaway Peninsula. The tidal range averages about 1.5 m at the mouth, decreasing to 1 m mid-estuary and increasing to 1.5 m at the head of tides (Ralston et al. 2019). The salinity intrusion varies from about 40 rkm during high river discharge to 120 rkm during low discharge (Bowen and Geyer 2003; Ralston et al. 2008).

The primary ETM in the Hudson is located near 20 rkm, formed by bottom salinity fronts associated with a constriction (Geyer et al. 2001; Traykovski et al. 2004). During moderate and low discharge, a secondary ETM forms near 55 rkm (Nitsche et al. 2010; Ralston et al. 2012). In the primary ETM, near-bottom sediment concentrations can exceed 1 g $L^{-1}$, and concentrations are greater than 100 mg/L in much of the saline estuary. In the tidal river, sediment concentrations are generally less than 100 mg $L^{-1}$ and vary with river discharge and tidal forcing (Wall et al. 2008; Ralston and Geyer 2017). Sediment inputs come from the two largest tributaries, the Mohawk and Upper Hudson Rivers, which converge just above the tidal limit. Numerous smaller tributaries also discharge into the tidal Hudson, cumulatively increasing the sediment load by 30-70% (Wall et al. 2008).

### *2.2 Observations*

Turbidity data were collected from monitoring stations located along the estuary. Data were accessed through the Hudson River Environmental Conditions Observing System (www.hrecos.org), which organizes monitoring data from multiple partner organizations, and the Centralized Data Management Office (cdmo.baruch.sc.edu). Monitoring stations were at Schodack Island (located at 212 rkm, available 2008-2019, partner organization Cary Institute of Ecosystem Studies), Tivoli North Bay (156 rkm, 2000-2019, Hudson River National Estuarine Research Reserve, HRNERR), Norrie Point (132 rkm, 2008-2019, HRNERR), and Piermont (37 rkm, 2008-2019, Lamont-Doherty Earth Observatory) (Fig. 1). Under most forcing conditions, Piermont is in the saline estuary and the other three stations are in the tidal freshwater (Hoitink and Jay 2016). For convenience we refer to the estuary spanning the tidal freshwater and saline regions.

All stations recorded near-surface turbidity. Time series were processed for quality control based on visual inspection to remove spurious outliers or anomalous trends indicative of instrument fouling. The quality control removed 0.3% to 2.8% of the measurements, depending on the station. The Tivoli North Bay sensor is located in a small channel connecting to a side embayment, so we only used measurements during flood tides. Daily median turbidity values were used to minimize the influence of individual bad measurements on longer term variability. At Tivoli, water samples were collected, filtered, dried, and weighed to measure suspended solids concentration for comparison with turbidity. The regression slope for total suspended solids (mg $L^{-1}$) was 1.2 times the turbidity (NTU, $r^2 = 0.52$, n = 219). Turbidity sensors at the other stations were not calibrated to SSC, but previous studies have also found calibrations with slopes of around 1 (Ralston et al. 2013; Ralston and Geyer 2017).

Volumetric discharge ($Q_r$) and sediment discharge ($Q_s$) measurements were collected from USGS gauging stations on the Mohawk and Upper Hudson. The Mohawk (at Cohoes, #01357500) has volumetric discharge 1917-2019 and sediment discharge for 1954-1959, 1976-1979, and 2002-2019. The Upper Hudson (Waterford, 01335770) has volumetric discharge 1887-1956 and 1976-2019, and sediment discharge 1976-2014. Mean daily mean SSC were calculated with $SSC = Q_s/Q_r$.

Turbidity was related to $Q_r$ by locally weighted scattered smoothing, or LOWESS (Cleveland 1979; Helsel and Hirsch 2002). The LOWESS approach has been used for sediment discharge rating curves in

rivers, including in trend analyses following discharge events (Warrick et al. 2013; Gray 2018). LOWESS regressions were calculated for log-transformed discharge and turbidity with a smoothing factor of 0.25. A bias correction factor was included to calculate turbidity from discharge using the regression (Ferguson 1986; Cohn 1995), with the form $C = 10\text{^}(C_{out} + \sigma^2/2)$, where $C_{out}$ is the output from the LOWESS regression to $\log_{10}(Q_r)$ and $\sigma^2$ is the variance in the residual. The variance in the residual was calculated in fractional subsets of $Q_r$ similar to the LOWESS smoothing factor to account for variability in the regression fit.

## 3. Results

Over the observation period (2008-2019), Irene and Lee accounted for the highest river discharge and observed turbidity (Fig. 1). The turbidity during and immediately following the 2011 events was greatest in the upper tidal river at Schodack Island, with 1000 NTU during Irene and 500 NTU during Lee. At the other stations in the tidal river, Tivoli North Bay and Norrie Point, turbidity was 200-300 NTU during the events. Increased turbidity was recorded during other high discharge periods, including spring freshets in 2013, 2014, and 2016, but those maxima were less than half the levels during Irene. In the saline estuary, the Piermont station was not operational during the 2011 events. During other years, the maximum turbidity at Piermont was typically around 100 NTU, with generally higher turbidity during the winter and spring and lower in the summer.

Turbidity from the four stations is plotted against discharge, and all the locations have positive slopes (Fig. 2). At Schodack Island, the turbidity dependence on discharge has a form similar to many rivers (Nash 1994), with a greater slope at higher discharge ($Q_r > 400$ m$^3$ s$^{-1}$), and weaker dependence at lower $Q_r$. Schodack is in a shallow and sandy part of the tidal river (Nitsche et al. 2007; Collins and Miller 2012), so resuspension of fine sediment is limited and turbidity varies strongly with river inputs. The slightly negative slope at low discharge may be an artifact of limited data, or may be due to increased organic particles during summer low discharge (Ralston and Geyer 2017). Turbidities at the Tivoli and Norrie Point stations that are farther seaward increase more gradually with discharge (Fig. 2b,c). Discharge varies annually by about an order of magnitude, and turbidity in the tidal river varies by more than an order of magnitude. The turbidity variability in the tidal freshwater is greater than that in the saline estuary, where the annual range typically spans a factor of 2-3 (Bokuniewicz and Arnold 1984; Ralston et al. 2012; Ralston and Geyer 2017). Correspondingly, the turbidity-discharge regression at Piermont has a narrower range the tidal river stations, and the discharge dependence is weaker (Fig. 2d).

Scatter in the turbidity-discharge relationships is due to the many processes that affect turbidity in addition to discharge. Sediment resuspension and trapping can vary with tidal amplitude, salinity, wind, and bed sediment properties. Lags in sediment transport can be weeks to months (Ralston and Geyer 2009; Ralston and Geyer 2017), distorting the correspondence between the daily discharge and turbidity along the estuary. Antecedent discharge conditions affect sediment availability in the estuary, with fine sediment accumulating during higher discharge and increasing tidal resuspension, potentially changing the relationship with daily discharge (Wall et al. 2008).

To evaluate whether inputs from Irene and Lee affected sediment availability in the estuary and thus turbidity over longer time scales, the turbidity vs. discharge relationship is considered on a yearly basis. Turbidity time series are segmented by water year (October 1-September 30) to reflect the seasonality of higher discharge in the late fall, winter, and spring and typically lower discharge summer. As an example, multiple years are shown for Tivoli North Bay (Fig. 3). Clustering of median daily observations above or below the LOWESS fit of the full 12-year record represents a shift in the turbidity-discharge relationship. Increased sediment availability following Irene and Lee corresponds to higher than average turbidity (for

a given discharge) in 2012 and 2013, as well as a few anomalously high turbidity observations during water year 2011 (Fig. 3d,e). In contrast, turbidity tends to be less than the long-term regression for most discharge conditions in 2015 (Fig. 3g).

Over the turbidity observation period, the combined annual average discharge from Upper Hudson and Mohawk Rivers varied by almost a factor of 2, from 350 $m^3 s^{-1}$ to 650 $m^3 s^{-1}$, and the maximum combined daily discharge varied by about a factor of 3, from 1460 $m^3 s^{-1}$ to 4460 $m^3 s^{-1}$ (Fig. 4a). Annual sediment inputs from the rivers were calculated based on observed discharge and regressions to long-term sediment discharge observations (Ralston et al. 2020), since the direct measurements of sediment discharge did not span the full period (Fig. 4b). The most notable variability in sediment inputs over this period was the large increase from the Mohawk with the storm events in 2011.

Annual averages of turbidity in the tidal freshwater and saline estuary varied by about a factor of 2 over the same period (Fig. 4c). The interannual variability in average turbidity is in part due to variation in river discharge, with higher turbidity during years with greater average discharge. However, the goal here is to assess whether hysteresis in the turbidity-discharge relationship may also contribute. To quantify this, we calculate the annual average of the ratio of the measured turbidity to that predicted by the turbidity-discharge regressions shown in Fig. 2. This turbidity ratio represents the factor by which the turbidity differed from the long-term regression, accounting for interannual variations in discharge (Fig. 4d). Discretization at periods shorter than a year were also examined, with similar (but noisier) results.

The interannual variation in the turbidity relative to the long-term regression was coherent among the three tidal freshwater stations (i.e. Schodack, Tivoli, and Norrie Point), despite separation of about 80 km and differences in local bed sediment. In 2012 and 2013, turbidity at all 3 locations was greater than expected based on the long-term regression, by factors of about 1.4 at Schodack, 1.3 at Tivoli, and 1.5 at Norrie. In 2010 and prior years, the turbidity factors were close to or less than 1 at all three stations. After 2013, the turbidity ratio returned to values similar to 1, representing a return to long-term average conditions, with values less than 1 before and after 2011-2014 potentially explained by the long-term regression including the elevated turbidity from Irene and Lee. Average turbidity in the tidal river thus depended both on $Q_r$ that year and on hysteresis in the turbidity-discharge relationship. For example, the mean $Q_r$ in 2012 (390 $m^3 s^{-1}$) was less than average (460 $m^3 s^{-1}$), and yet the average turbidity that year was the second highest overall (Fig. 4c). In 2013 the turbidity increased in part because the discharge increased, but also because of the above-average turbidity-discharge relationship (Fig. 4d).

Another approach to characterizing the temporal variability in the turbidity-discharge relationship is to calculate the slope of the cumulative residual between the observed and predicted turbidity (Gray 2018). Periods when observed turbidity was greater than expected have a positive slope for the cumulative residual, and periods with turbidity less than expected have a negative slope. Results using the cumulative residual slopes are consistent with the turbidity ratios, with positive slopes during years with turbidity ratio greater than 1 and negative residuals for turbidity ratios less than 1 (Suppl. Fig. 1). Similarly, the cumulative residual slopes at the tidal river stations are maximum in 2012 and 2013, after Irene and Lee, and decrease to zero or negative values in 2014 or 2015.

The temporal variability in the turbidity-discharge relationship was coherent among the freshwater tidal stations, but observations in the saline estuary did not exhibit the same interannual response (Fig. 4c). For example, the turbidity ratio at Tivoli was strongly correlated with that at Norrie Point ($r^2 = 0.93$, $p<0.001$, $n=11$) and had a weaker correlation with Schodack Island ($r^2 = 0.63$, $p=0.028$, $n=12$), but the correlation with Piermont in the saline estuary was not significant ($r^2 = 0.33$, $p=0.35$, $n=10$). The Piermont station

exhibited only a modest increase in the turbidity ratio in 2012 after Irene and Lee (with a data gap in 2013), and in general has less variability in the turbidity-discharge relationship.

The turbidity ratios in the estuary were not significantly correlated with the year-to-year variability in the sediment mass inputs from the Mohawk and Upper Hudson (Fig. 4b). We also calculated the residual of the LOWESS regressions of $\log_{10}(SSC)$ vs. $\log_{10}(Q_r)$ for the tributaries on an annual basis. Precipitation from Irene and Lee was much greater in the Mohawk watershed than the Upper Hudson (Lumia et al. 2014), so increased sediment availability following the events may be expected to alter the sediment-discharge relationship of the Mohawk. In water years 2012-2014 following the events, the average *SSC* in the Mohawk did increase by a factor of about 1.2 above the regression values, but the Mohawk turbidity ratio was not significantly correlated with the turbidity ratios in the estuary. As expected from precipitation patterns during Irene-Lee, the turbidity-discharge ratio for the Upper Hudson did not change post-flood.

## 4. Summary and discussion

Long-term monitoring data allow for characterization of turbidity-discharge relationships in the estuary that might be obscured by variability at tidal to seasonal time scales. In the tidal freshwater, turbidity depended strongly on discharge (Fig. 2). Average residuals between observed turbidity and that predicted from the discharge regressions were coherent among stations in the tidal river, with increased turbidity in the 2 years following tropical storms Irene and Lee (Fig. 4). Variations in the turbidity residuals in the estuary were not directly tied to the interannual sediment inputs from tributaries, which suggests that increased sediment availability for resuspension after the events led to hysteresis in the sediment-discharge relationship. The coherence among stations separated by 80 km suggests that the signal is also not predominantly due to local inputs from a particular tributary.

Increased turbidity suggests an increase in SSC, particularly for a fixed particle size distribution. Alternatively, temporal decreases in the dominant particle size could increase turbidity and change the relationship to SSC (Downing 2006). Seasonal variation in the slope between turbidity and SSC of about a factor of 2 has been noted in the tidal Hudson, likely due to changes in particle size with discharge (Ralston and Geyer 2017). Thus the shift toward higher turbidity ratios may reflect a combination of greater availability and finer grain size following discharge events (Yellen et al. 2016).

The turbidity responses differed between the tidal river and saline estuary, where changes in the turbidity-discharge relationship were less apparent following the discharge events. In the tidal river, SSC tends to be lower and the bed less muddy than in the saline estuary (Nitsche et al. 2007). The sediment available for resuspension at event to seasonal time scales has been termed the mobile sediment pool (Wellershaus 1981; Schoellhamer 2011; Geyer and Ralston 2018). While the size of the mobile pool is difficult to quantify, the persistent increase in turbidity in the tidal river following Irene and Lee suggests that the sediment input represented a major increase in the size of the mobile pool. About 2/3 of the sediment input by the events remained in the tidal river several months after the events (Ralston et al. 2013), and the 2-year period of increased turbidity may be indicative of the time scale for the tidal river to adjust back to pre-storm conditions.

In the saline estuary, turbidity on average is greater, the bed is muddier, and the mobile pool is larger than in the tidal river. Previous studies have highlighted the seasonal to annual variation in SSC and deposition (Geyer et al. 2001; Woodruff et al. 2001). Observations in the lower ETM found that the freshets in 1998 and 1999 each deposited about 0.3 Mt of new sediment, despite large differences in the watershed sediment inputs in those years (Woodruff et al. 2001). This decoupling between deposition in the ETM and the watershed inputs is consistent with the limited variability in the turbidity-discharge residual at

Piermont. If the mobile pool in the saline estuary is many times the annual average input, then the fractional increase from Irene and Lee may be minor. Similarly, in San Francisco Bay a decrease in sediment supply associated with dam construction did not affect sediment concentrations until decades later, first in the tidal freshwater Delta and subsequently in the saline estuary (Schoellhamer 2011; Hestir et al. 2013; Schoellhamer et al. 2013). In the Penobscot estuary, the mobile sediment pool was estimated to be 6-8 times the annual average input based on recovery time scales following a contaminant release (Geyer and Ralston 2018).

Differences between the tidal river and saline estuary in the hysteresis of the turbidity-discharge relationships reflect the relative coupling between sediment supply and river discharge. In the saline estuary, the mobile pool is large compared to the annual supply, such that a major discharge event does not drastically increase sediment availability. In contrast, fine grained bed sediment in the tidal river is more limited, so event inputs represent a fractionally bigger change, and turbidity is increased for a couple of years as the added sediment gradually moves seaward and deposits in lower energy shoals and wetlands (Ralston and Geyer 2017; Yellen et al. 2020). For comparison, the hysteresis in turbidity-discharge relationship in the tidal river is shorter in duration than observed in rivers along the U.S. West Coast, where sediment concentrations remained elevated for 5 years or longer after events (Warrick et al. 2013; Gray 2018). Long-term measurements at stream gauging stations allow for assessment of the variability in turbidity/sediment-discharge relationships in the watershed, but such long-term measurements are far less common in estuaries. These results point to the utility of such measurements for assessing the multiple time scales of sediment variability in other estuaries.

## Acknowledgements

This work was sponsored by the National Estuarine Research Reserve System Science Collaborative, funded by the National Oceanic and Atmospheric Administration and managed by the University of Michigan Water Center (NAI4NOS4190145). The data used in this study were all downloaded from publicly available sources (USGS, HRECOS, or CDMO) as described in the Methods section.

## References

Ahn, Kuk-Hyun, Brian Yellen, and Scott Steinschneider. 2017. Dynamic linear models to explore time-varying suspended sediment-discharge rating curves. *Water Resources Research* 53: 4802–4820.

Bokuniewicz, Henry J., and Chester L. Arnold. 1984. Characteristics of suspended sediment transport in the lower Hudson River. *Northeastern Environmental Science* 3: 184–189.

Bowen, Melissa M., and W. Rockwell Geyer. 2003. Salt transport and the time-dependent salt balance of a partially stratified estuary. *Journal of Geophysical Research* 108: 3158. doi:10.1029/2001JC001231.

Burchard, Hans, Henk M. Schuttelaars, and David K. Ralston. 2018. Sediment Trapping in Estuaries. *Annual Review of Marine Science* 10: null. doi:10.1146/annurev-marine-010816-060535.

Cleveland, William S. 1979. Robust locally weighted regression and smoothing scatterplots. *Journal of the American statistical association* 74: 829–836.

Cohn, T. A. 1995. Recent advances in statistical methods for the estimation of sediment and nutrient transport in rivers. *Reviews of Geophysics* 33: 1117–1123. doi:10.1029/95RG00292.

Collins, M. J., and D. Miller. 2012. Upper Hudson River Estuary (usa) Floodplain Change Over the 20th Century. *River Research and Applications* 28: 1246–1253. doi:10.1002/rra.1509.

Dalrymple, Robert W., and Kyungsik Choi. 2007. Morphologic and facies trends through the fluvial–marine transition in tide-dominated depositional systems: a schematic framework for environmental and sequence-stratigraphic interpretation. *Earth-Science Reviews* 81: 135–174.

Dethier, Evan, Francis J. Magilligan, Carl E. Renshaw, and Keith H. Nislow. 2016. The role of chronic and episodic disturbances on channel–hillslope coupling: the persistence and legacy of extreme floods. *Earth Surface Processes and Landforms* 41: 1437–1447.

Downing, John. 2006. Twenty-five years with OBS sensors: The good, the bad, and the ugly. *Continental Shelf Research* 26. Special Issue in Honor of Richard W. Sternberg's Contributions to Marine Sedimentology: 2299–2318. doi:10.1016/j.csr.2006.07.018.

Ferguson, R. I. 1986. River loads underestimated by rating curves. *Water resources research* 22: 74–76.

Geyer, W. Rockwell, and D. K. Ralston. 2018. A mobile pool of contaminated sediment in the Penobscot Estuary, Maine, USA. *Science of The Total Environment* 612: 694–707. doi:10.1016/j.scitotenv.2017.07.195.

Geyer, W. Rockwell, Jonathan D. Woodruff, and Peter Traykovski. 2001. Sediment Transport and Trapping in the Hudson River Estuary. *Estuaries* 24: 670–679.

Gray, A. B., J. A. Warrick, G. B. Pasternack, E. B. Watson, and M. A. Goñi. 2014. Suspended sediment behavior in a coastal dry-summer subtropical catchment: Effects of hydrologic preconditions. *Geomorphology* 214: 485–501. doi:10.1016/j.geomorph.2014.03.009.

Gray, Andrew B. 2018. The impact of persistent dynamics on suspended sediment load estimation. *Geomorphology* 322: 132–147.

Helsel, Dennis R., and Robert M. Hirsch. 2002. *Statistical methods in water resources*. Vol. 323. US Geological Survey Reston, VA.

Hestir, Erin L., David H. Schoellhamer, Tara Morgan-King, and Susan L. Ustin. 2013. A step decrease in sediment concentration in a highly modified tidal river delta following the 1983 El Niño floods. *Marine Geology* 345. A Multi-Discipline Approach for Understanding Sediment Transport and Geomorphic Evolution in an Estuarine-Coastal System: San Francisco Bay: 304–313. doi:10.1016/j.margeo.2013.05.008.

Hoitink, A. J. F., and D. A. Jay. 2016. Tidal river dynamics: Implications for deltas. *Reviews of Geophysics* 54: 2015RG000507. doi:10.1002/2015RG000507.

Lumia, Richard, Gary D. Firda, and Travis L. Smith. 2014. *Floods of 2011 in New York*. US Department of the Interior, US Geological Survey.

McHale, Michael R., and Jason Siemion. 2014. *Turbidity and suspended sediment in the upper Esopus Creek watershed, Ulster County, New York*. Scientific Investigations Report 2014–5200. U.S. Geological Survey.

Morehead, Mark D., James P. Syvitski, Eric WH Hutton, and Scott D. Peckham. 2003. Modeling the temporal variability in the flux of sediment from ungauged river basins. *Global and Planetary change* 39: 95–110.

Nash, D. B. 1994. Effective sediment-transporting discharge from magnitude-frequency analysis. *Journal of Geology* 102: 79–96.

Nitsche, F.O., T.C. Kenna, and M. Haberman. 2010. Quantifying 20th century deposition in complex estuarine environment: An example from the Hudson River. *Estuarine, Coastal and Shelf Science* 89: 163–174. doi:10.1016/j.ecss.2010.06.011.

Nitsche, F.O., W.B.F. Ryan, S.M. Carbotte, R.E. Bell, A. Slagle, C. Bertinado, R. Flood, T. Kenna, and C. McHugh. 2007. Regional patterns and local variations of sediment distribution in the Hudson River Estuary. *Estuarine, Coastal and Shelf Science* 71: 259–277. doi:10.1016/j.ecss.2006.07.021.

Postma, H. 1961. Transport and accumulation of suspended matter in the Dutch Wadden Sea. *Netherlands Journal of Sea Research* 1: 148–180.

Ralston, David K., and W. Rockwell Geyer. 2009. Episodic and Long-Term Sediment Transport Capacity in The Hudson River Estuary. *Estuaries and Coasts* 32: 1130–1151. doi:10.1007/s12237-009-9206-4.

Ralston, David K., and W. Rockwell Geyer. 2017. Sediment transport time scales and trapping efficiency in a tidal river. *Journal of Geophysical Research: Earth Surface* 122: 2042–2063.

Ralston, David K., W. Rockwell Geyer, and James A. Lerczak. 2008. Subtidal Salinity and Velocity in the Hudson River Estuary: Observations and Modeling. *Journal of Physical Oceanography* 38: 753–770.

Ralston, David K., W. Rockwell Geyer, and John C. Warner. 2012. Bathymetric controls on sediment transport in the Hudson River estuary: Lateral asymmetry and frontal trapping. *Journal of Geophysical Research* 117: C10013. doi:10.1029/2012JC008124.

Ralston, David K., Stefan Talke, W. Rockwell Geyer, Hussein A. M. Al-Zubaidi, and Christopher K. Sommerfield. 2019. Bigger Tides, Less Flooding: Effects of Dredging on Barotropic Dynamics in a Highly Modified Estuary. *Journal of Geophysical Research: Oceans* 124: 196–211. doi:10.1029/2018JC014313.

Ralston, David K., John C. Warner, W. Rockwell Geyer, and Gary R. Wall. 2013. Sediment transport due to extreme events: The Hudson River estuary after tropical storms Irene and Lee. *Geophysical Research Letters* 40: 2013GL057906. doi:10.1002/2013GL057906.

Ralston, David K., Brian Yellen, and Jonathan D. Woodruff. 2020. Watershed sediment supply and potential impacts of dam removals for an estuary. Submitted manuscript. DOI: 10.1002/essoar.10502519.1. ESSOAr.

Schoellhamer, David H. 2011. Sudden Clearing of Estuarine Waters upon Crossing the Threshold from Transport to Supply Regulation of Sediment Transport as an Erodible Sediment Pool is Depleted: San Francisco Bay, 1999. *Estuaries and Coasts* 34: 885–899. doi:10.1007/s12237-011-9382-x.

Schoellhamer, David H., Scott A. Wright, and Judith Z. Drexler. 2013. Adjustment of the San Francisco estuary and watershed to decreasing sediment supply in the 20th century. *Marine Geology* 345: 63–71.

Sommerfield, Christopher K., Daniel I. Duval, and Robert J. Chant. 2017. Estuarine sedimentary response to Atlantic tropical cyclones. *Marine Geology* 391: 65–75. doi:10.1016/j.margeo.2017.07.015.

Syvitski, James P., Mark D. Morehead, David B. Bahr, and Thierry Mulder. 2000. Estimating fluvial sediment transport: The rating parameters. *Water Resources Research* 36: 2747–2760. doi:10.1029/2000WR900133.

Traykovski, Peter, W. Rockwell Geyer, and Chris Sommerfield. 2004. Rapid sediment deposition and fine-scale strata formation in the Hudson estuary. *Journal of Geophysical Research* 109: F02004. doi:10.1029/2003JF000096.

Wall, G., E. Nystrom, and S. Litten. 2008. Suspended Sediment Transport in the Freshwater Reach of the Hudson River Estuary in Eastern New York. *Estuaries and Coasts*. doi:10.1007/s12237-008-9050-y.

Walling, D. E. 1977. Assessing the accuracy of suspended sediment rating curves for a small basin. *Water Resources Research* 13: 531–538.

Walling, Desmond E., Philip N. Owens, and Graham J. L. Leeks. 1998. The role of channel and floodplain storage in the suspended sediment budget of the River Ouse, Yorkshire, UK. *Geomorphology* 22: 225–242. doi:10.1016/S0169-555X(97)00086-X.

Warrick, J. A., Mary Ann Madej, M. A. Goñi, and R. A. Wheatcroft. 2013. Trends in the suspended-sediment yields of coastal rivers of northern California, 1955–2010. *Journal of hydrology* 489: 108–123.

Warrick, Jonathan A., and David M. Rubin. 2007. Suspended-sediment rating curve response to urbanization and wildfire, Santa Ana River, California. *Journal of Geophysical Research: Earth Surface* 112.

Wellershaus, St. 1981. Turbidity maximum and mud shoaling in the Weser estuary. *Archiv fur Hydrobiologie* 92.

Woodruff, Jonathan D., W. Rockwell Geyer, Christopher K. Sommerfield, and Neal W. Driscoll. 2001. Seasonal variation of sediment deposition in the Hudson River estuary. *Marine Geology* 179: 105–119. doi:10.1016/S0025-3227(01)00182-7.

Yellen, B., J. D. Woodruff, L. N. Kratz, S. B. Mabee, J. Morrison, and A. M. Martini. 2014. Source, conveyance and fate of suspended sediments following Hurricane Irene. New England, USA. *Geomorphology* 226: 124–134.

Yellen, Brian, Jonathan D. Woodruff, Timothy L. Cook, and Robert M. Newton. 2016. Historically unprecedented erosion from Tropical Storm Irene due to high antecedent precipitation. *Earth Surface Processes and Landforms* 41: 677–684. doi:10.1002/esp.3896.

Yellen, Brian, Jonathan D. Woodruff, Caroline Ladlow, David K. Ralston, Sarah Fernald, and Waverly Lau. 2020. Rapid Tidal Marsh Development in Anthropogenic Backwaters. EarthArXiv.

411 **Figures**

Figure 1

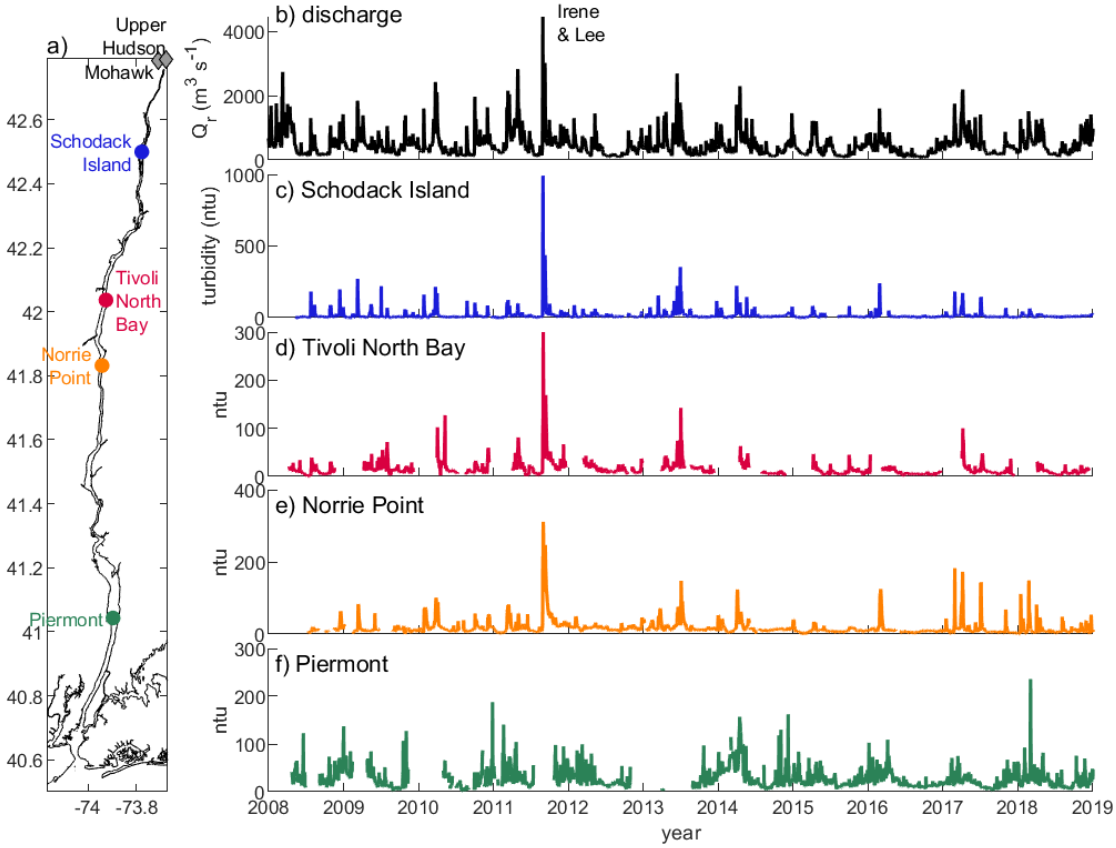


412

413 **Figure 1.** Turbidity at monitoring stations along the estuary. a) Station locations, b) daily average
414 discharge from the Upper Hudson and Mohawk, noting Tropical Storms Irene and Lee in 2011, c-f) daily
415 median turbidity from Schodack Island, Tivoli North Bay, Norrie Point, and Piermont.

Figure 2

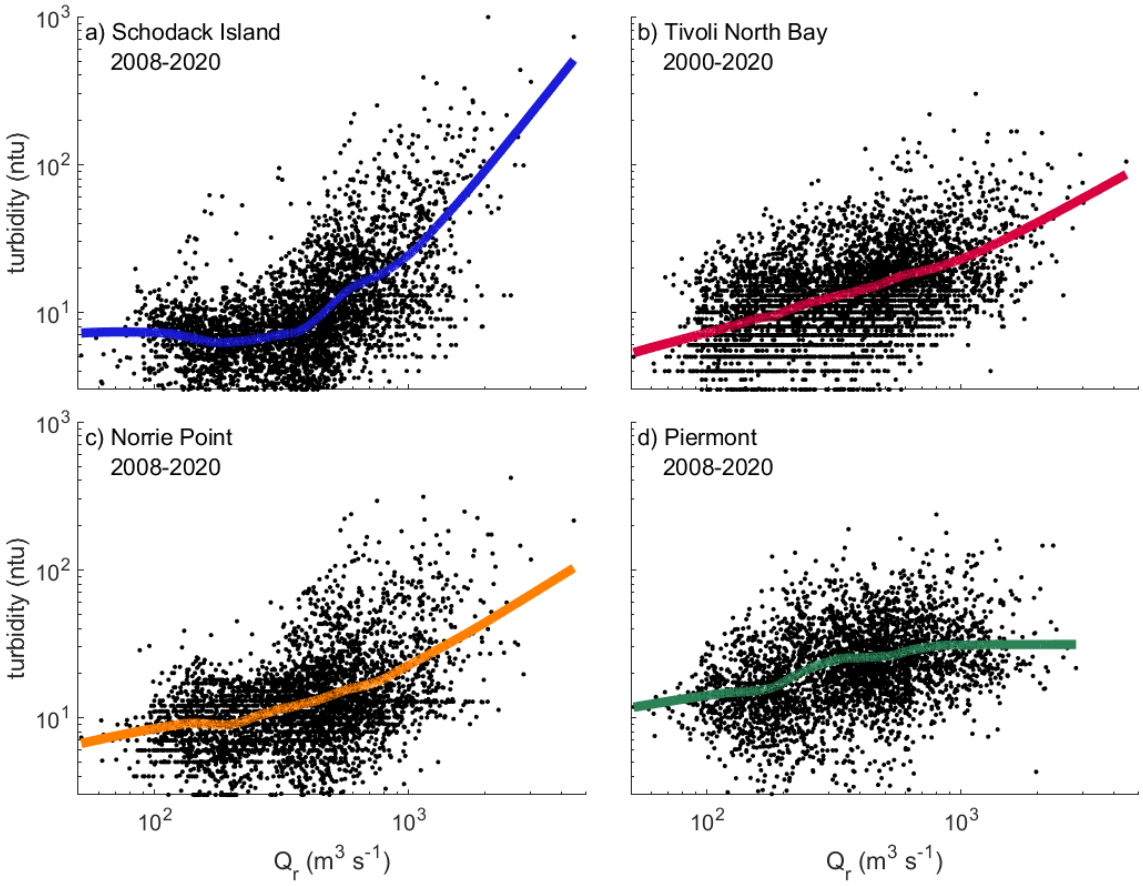


416

417 **Figure 2.** Turbidity vs. river discharge a) at Schodack Island, b) Tivoli North Bay, c) Norrie Point, and d)
418 Piermont. Daily turbidity data are in black and LOWESS regressions are colored.

Figure 3

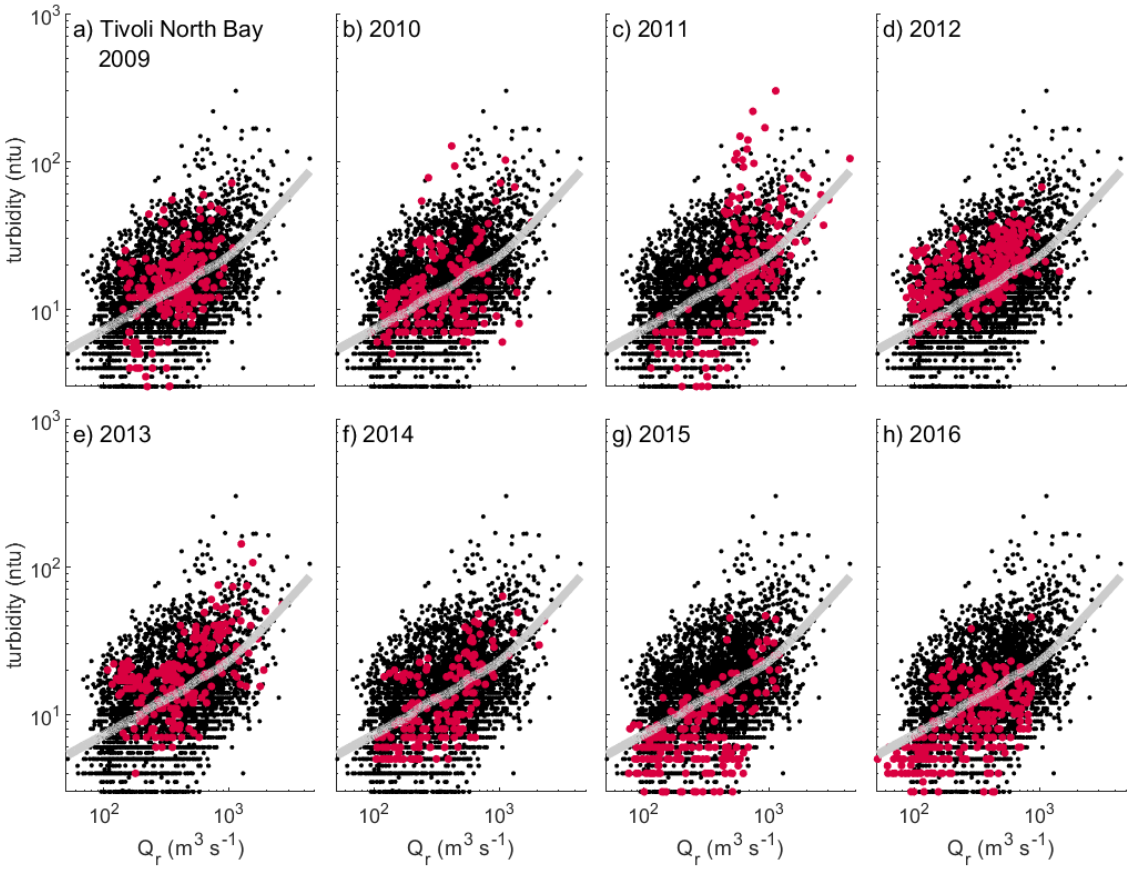


**Figure 3.** Turbidity vs. river discharge at Tivoli North Bay by water year from 2009 to 2016. The full record is in black, and data for each year are colored. The LOWESS fit to the full record is gray.

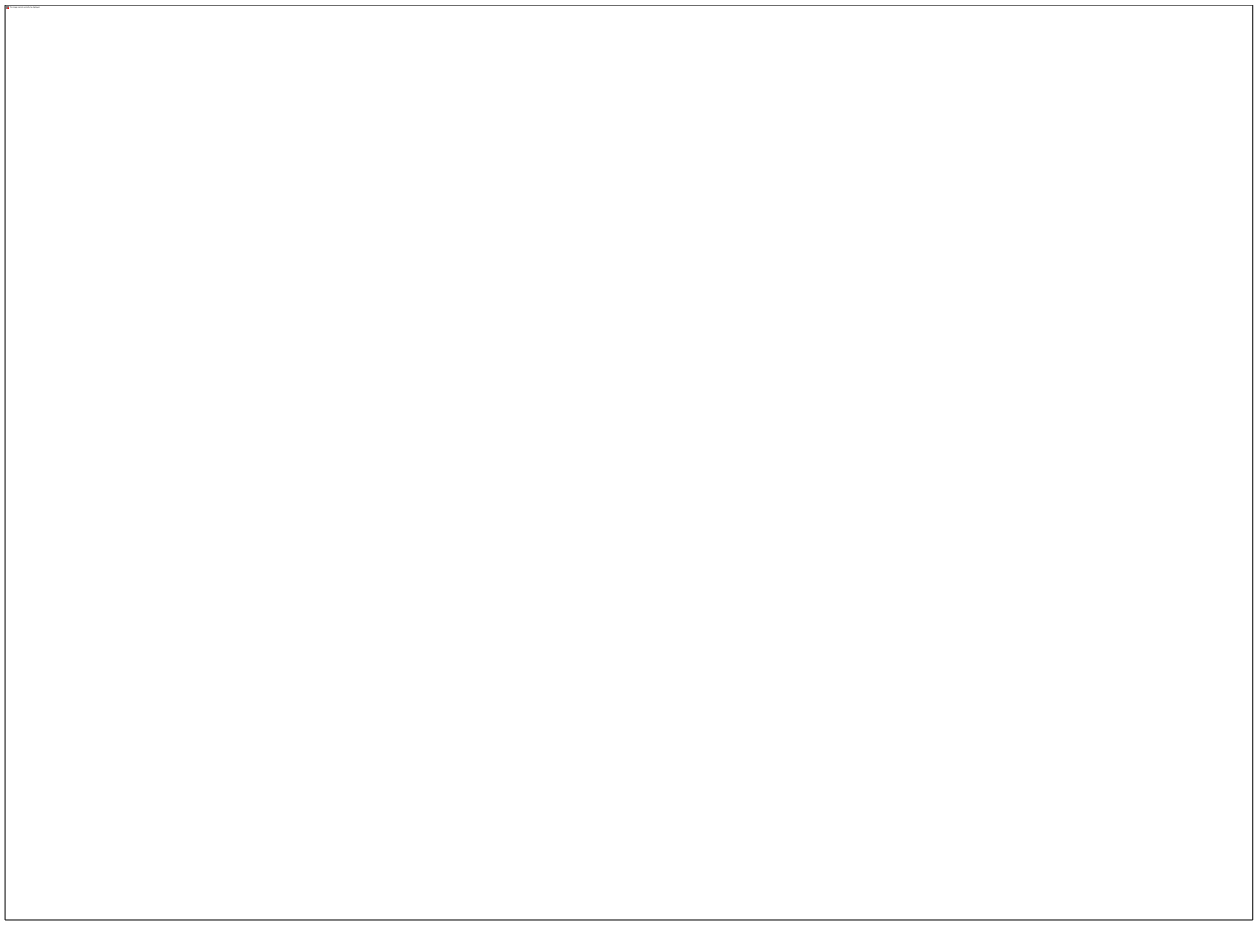

**Figure 4.** Discharge and turbidity by water year. a) Mean and maximum discharge of the Upper Hudson and Mohawk rivers, b) annual sediment input from the Mohawk and Upper Hudson, c) annual average turbidity in the tidal river and estuary, d) annual average of the ratio of measured turbidity to that predicted by the long-term $Q_r$ regressions (Fig. 2).

S1

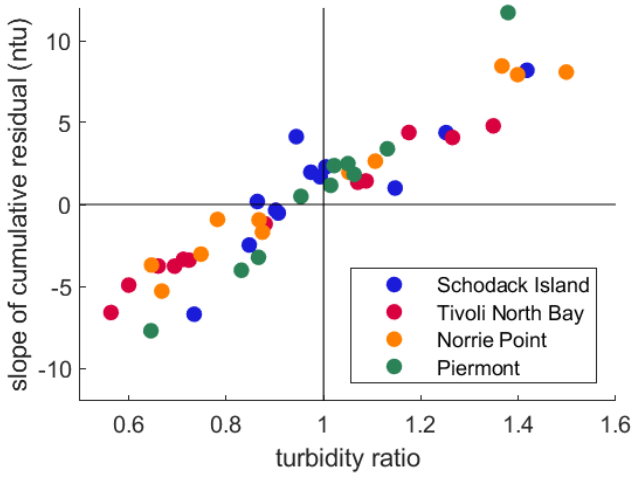

**Figure S1.** Annual averages of the slope of the cumulative residual vs. turbidity ratio. Turbidity ratio same as in Fig. 4d. Positive slopes and turbidity ratios greater than 1 correspond with years when the turbidity vs. discharge relationship was greater than the long-term regression.

**Figure 1.**

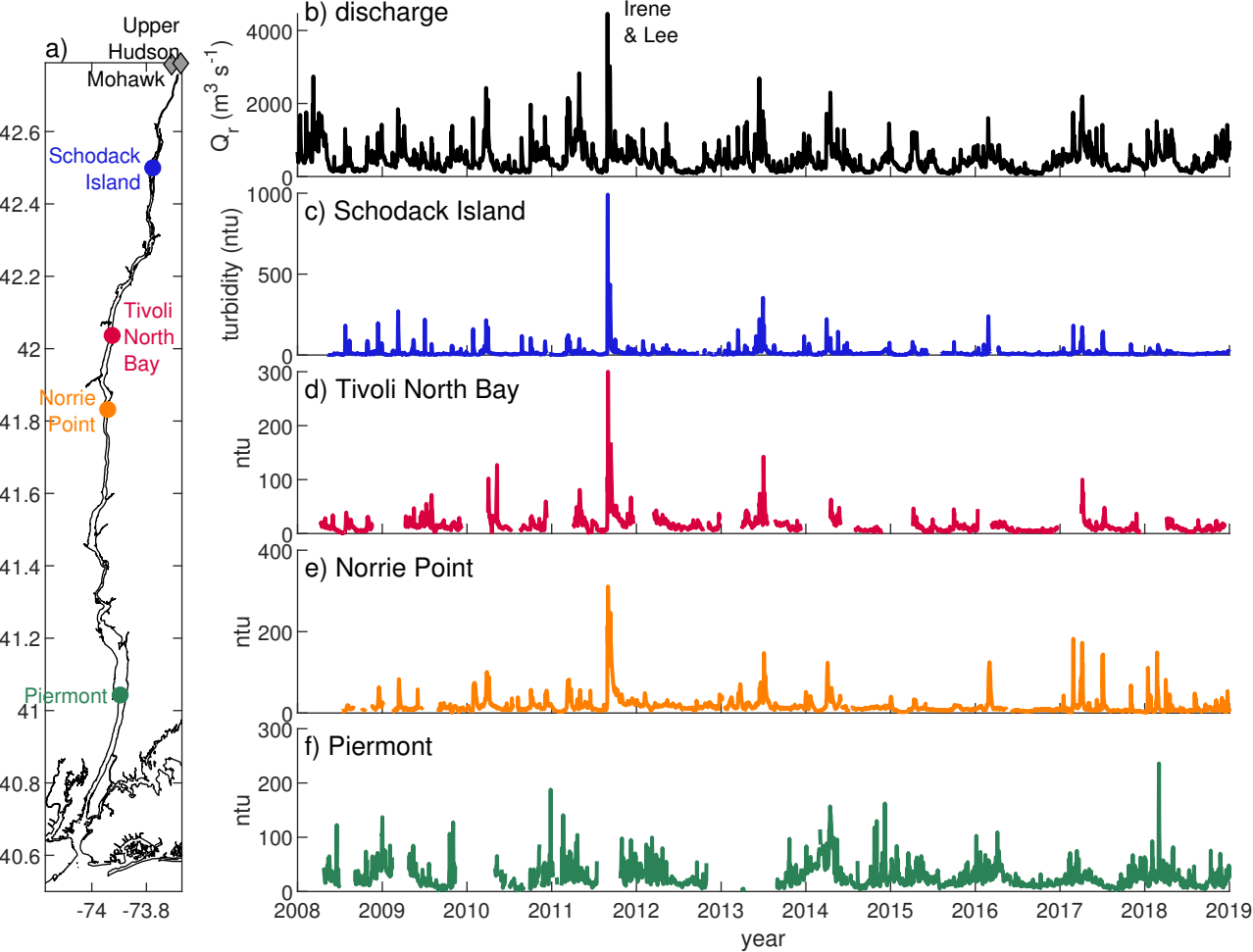
a)
Upper Hudson
Mohawk
Schodack Island
Tivoli North Bay
Norrie Point
Piermont
42.6
42.4
42.2
42
41.8
41.6
41.4
41.2
41
40.8
40.6
-74
-73.8
b) discharge
Irene & Lee
$Q_r$ ($m^3$ $s^{-1}$)
4000
2000
0
c) Schodack Island
turbidity (ntu)
1000
500
0
d) Tivoli North Bay
ntu
300
200
100
0
e) Norrie Point
ntu
400
200
0
f) Piermont
ntu
300
200
100
0
2008
2009
2010
2011
2012
2013
2014
2015
2016
2017
2018
2019
year

**Figure 2.**

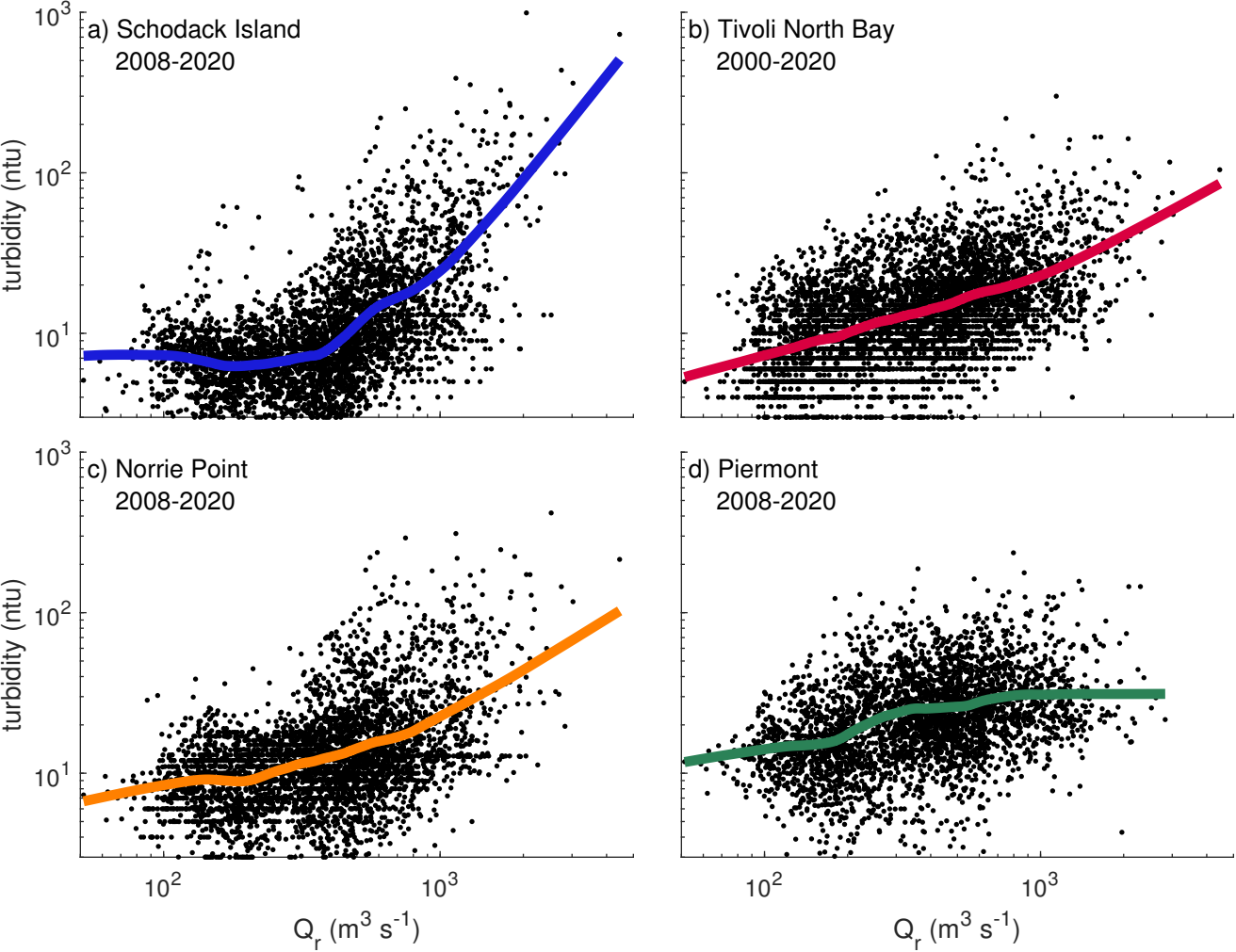
a) Schodack Island
2008-2020
b) Tivoli North Bay
2000-2020
c) Norrie Point
2008-2020
d) Piermont
2008-2020
turbidity (ntu)
$10^1$
$10^2$
$10^3$
$10^2$
$10^3$
$Q_r$ ($m^3$ $s^{-1}$)

**Figure 3.**

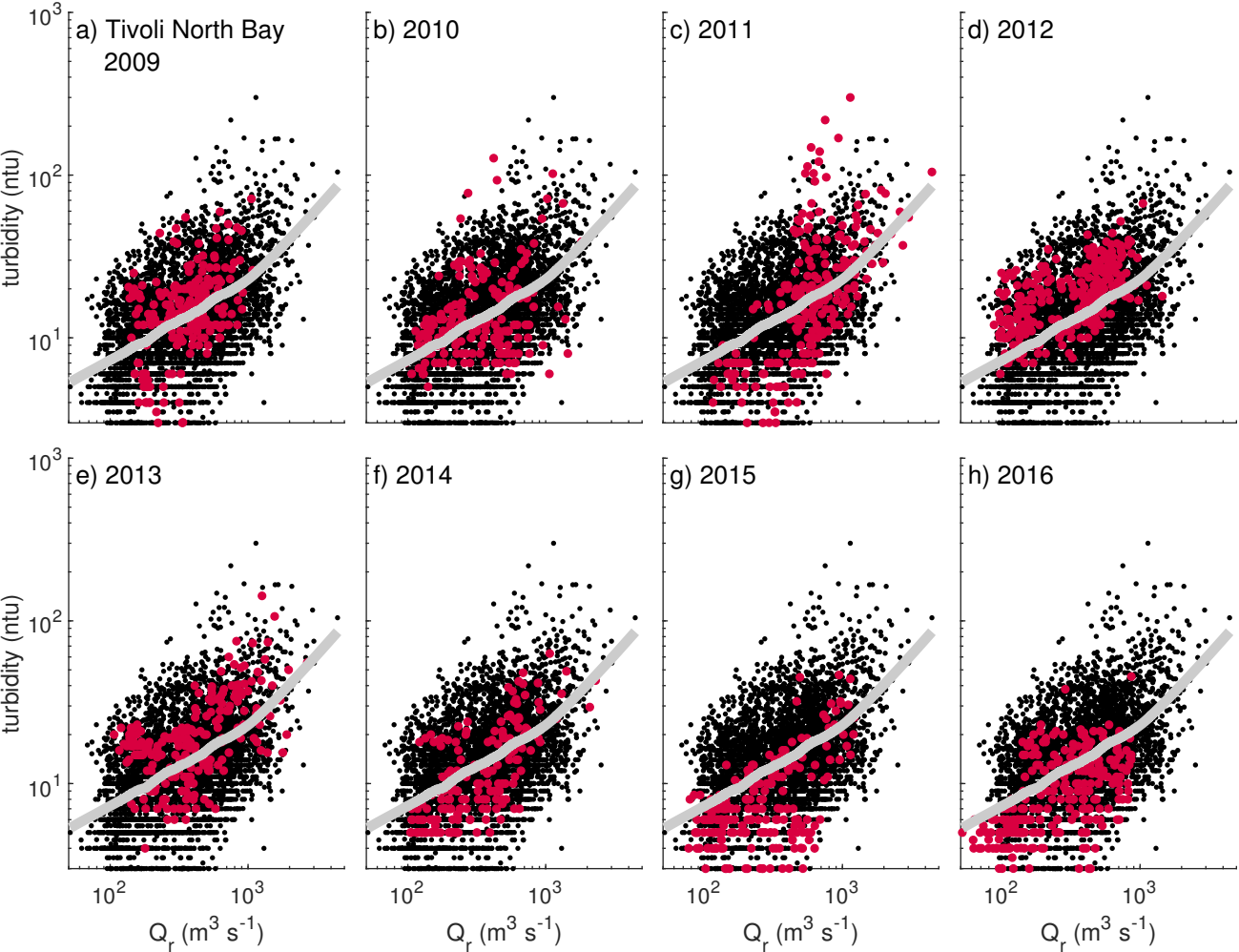
a) Tivoli North Bay
2009
b) 2010
c) 2011
d) 2012
e) 2013
f) 2014
g) 2015
h) 2016
turbidity (ntu)
$10^3$
$10^2$
$10^1$
$10^2$
$10^3$
$Q_r$ ($m^3$ $s^{-1}$)

**Figure 4.**

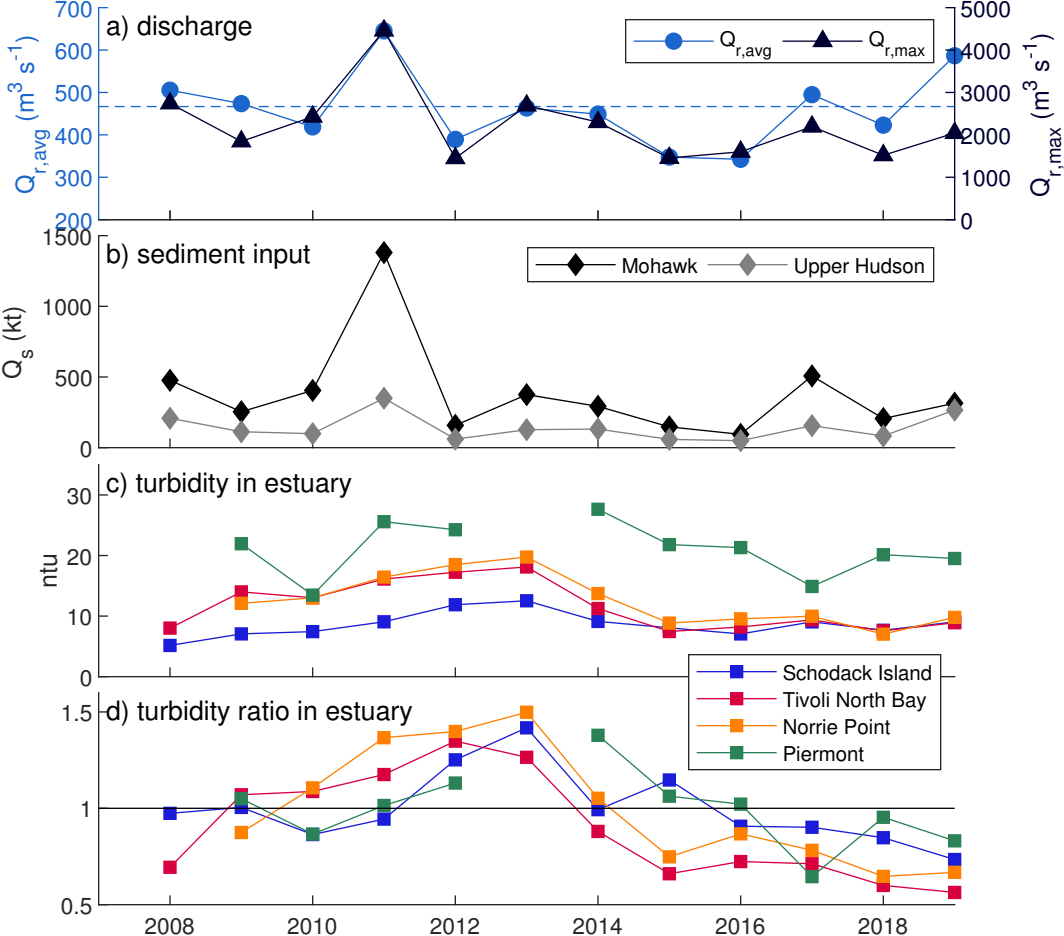
a) discharge
$Q_{r,avg}$
$Q_{r,max}$
$Q_{r,avg}$ ($m^3$ $s^{-1}$)
$Q_{r,max}$ ($m^3$ $s^{-1}$)
b) sediment input
Mohawk
Upper Hudson
$Q_s$ (kt)
c) turbidity in estuary
ntu
d) turbidity ratio in estuary
Schodack Island
Tivoli North Bay
Norrie Point
Piermont
2008
2010
2012
2014
2016
2018